UDC 550.34.01+66.011

G. Djolov[1], *Sc.D.*, **G. Fourie**[2], *Sc.D.*, **J. Pienaar**[3], *Sc.D.*
[1]*University of Pretoria, South Africa,*
[2]*SASOL Technology Research & Development, South Africa,*
[3]*North-West University (Potchefstroom Campus), South Africa*

MODELLING LONG-RANGE TRANSPORT AND CHEMICAL TRANSFORMATION OF POLLUTANTS IN SOUTHERN AFRICA REGION

Abstract. *The paper presents the results of long-range atmospheric model developed specifically for the Southern hemisphere conditions. The model utilizes a combined Eulerian-Lagrangian description of the transport and diffusion of pollutants, calculation of their chemical transformations, dry and wet deposition as well as the pH value of precipitation.*

Keywords: *long-range pollutants transport, atmospheric boundary layer, emission, surface roughness, meteorology, atmospheric chemistry, turbulent diffusion.*

1 Introduction

Dispersion modelling of transport, diffusion and chemical transformation of pollutants and trace gases over the region of southern Africa which spans between 52^o South to 1^o North, 28^o West to 68^o East, presents a special challenge due to three major factors. The first factor is associated with the frequent occurrence of a stable anticyclonic environment that inhibits the vertical exchange of air masses and stratifies the troposphere into persistent layers, in which residence times of pollutants are prolonged from several days to weeks over the region. The second factor stems from the different distribution of emission sources between the Northern and Southern hemispheres. Natural emissions from forest fires, vegetation, soils and domestic fires are equal or substantially bigger than fossil fuel emissions over larger parts of the studied region. Thirdly, long-range transport is vital for the existence/destruction of many fragile ecosystems that receive nutrients/pollutants mainly from the atmosphere.

In addition to these major factors one should keep in mind that experimental studies on the tropical meteorology factors affecting the long-range transport and chemical transformation of pollutants are very few, and theoretical understanding of the atmospheric processes in the regions with negligible Coriolis force, is not yet in place. Special attention should be placed on the identification of key linkages among the physical, chemical and anthropogenic processes underpinning the functioning of the bio-geophysical and bio-geochemical systems of Southern Africa that lead to significantly elevated ozone concentrations over considerable sections of the tropics.

2 Data and Methodology

2.1 Modelling Domain

The modelling domain implemented for this study extends from 10^{o}E to 40^{o}E and 10^{o}S to 35^{o}S as illustrated in Fig. 1. This region covers the southern part of Africa, including Angola (Ang), Namibia (Nam), Botswana (Bot), Zambia (Zam), Zimbabwe (Zim), Mozambique (Moz), Malawi (Mal) and South Africa (SA). A Cartesian grid was superimposed on the modelling domain. The 60x50 grid (3000 cells) was positioned to

conform to a 0.5° resolution on the modelling domain. An illustration of the superimposed Cartesian grid is shown in Fig. 1. This grid was utilized as a reference framework for all simulations in the Lagrangian-Eulerian Diffusion (LED) model.

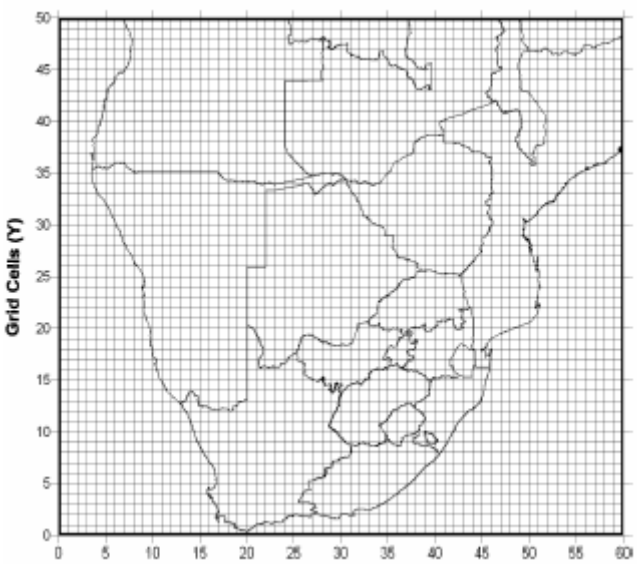

Fig. 1 – Modelling domain with the Cartesian grid implemented for LED.

2.2 The Lagrangian–Eulerian diffusion model

The Lagrangian–Eulerian Diffusion model utilizes in a complimentary way the positive features of the Lagrangian and Eulerian descriptions of hydrodynamic flows. Following the Lagrangian approach any volume of polluted air (puff) is identified by the trajectory of its center of mass. The diffusion and transformation processes of pollutants are investigated on the basis of analytical and numerical solutions of the appropriate differential equations in Eulerian coordinates with origin at the center of mass of puffs. Experiments and theoretical studies revealed the fundamental fact that the transport and diffusion of pollutants in the atmosphere can be investigated by separating the horizontal and vertical processes on the basis of the following formula:

$$C^K(x,y,z) = \sum_{i=1}^{M} \sum_{j=1}^{N_j} Q_{ij}^K(t_{ij}) q_h\left(x, x_{ij}^c, y, y_{ij}^c, t_{ij}\right) q_z\left(z, z_{ij}^c, t_{ij}\right) q_w\left(t_{ij}\right), \qquad (1)$$

where $C^K(x,y,z)$ -concentration of K pollutant in a point (x,y,z), $Q_{ij}^K(0)$ is the quantity of the K_{th} pollutant in the j_{th} puff emitted by the i_{th} source at the moment $t_{ij}=0$, M is the number of sources, N_j is the number of puffs, q_h and q_z are the horizontal and vertical distribution functions, q_w is the wash-out function, x_{ij}^c, y_{ij}^c, z_{ij}^c are the centres of coordinates and t_{ij} life time of the puff. The time variation of $Q_{ij}^K(0)$ is due to chemical transformations, dry and wet deposition processes. The analytical expressions for the functions q_h, q_z, q_w and more details for the LED model are presented in [2]. It should be pointed out that the vertical and horizontal diffusion functions are explicitly dependent on the atmospheric boundary layer

(ABL) turbulence through the eddy transfer coefficients in vertical and horizontal direction and wind velocity profile. Therefore, LED needs input from an appropriate simple enough and reliable ABL model which allows for incorporation of new research developments in the ABL dynamics.

2.3 Atmospheric boundary layer

A unique feature to LED, among the long-range models is the use of an appropriate ABL model calculating its dynamics and turbulent characteristics. Usually, the long range models are driven by the output of the best available mesoscale forecast models or in the diagnostic case by observed meteorological fields. In both cases, however, the ABL dynamics is not properly represented due to the restrictions in the model vertical resolution or insufficient number and distribution of observations. This is a serious simplification since the changes in wind velocity and atmospheric stability occurring in the ABL influence dramatically the transport and diffusion processes. Thus, for example, the value of the vertical exchange coefficient changes by order of magnitude depending on the stability conditions in the ABL. The magnitude and direction of the wind velocity vary considerably with height, and the angle between the geostrophic and surface wind can surpass 50-60 degrees. The wind variations are even more complicated when the ABL is affected by baroclinicity. Turbulent friction convergence creates vertical motions that in spite of their small value, lead to a substantial displacement of the polluted air volumes because of their perseverance. Another important consideration is that most of the emissions of pollutants and trace gases are released from sources located near the earth surface up to few hundred meters. The existence of frequent inversion layers at the top of ABL forces the diffusion and transport of pollutants to take place in the lower parts of the atmosphere for prolonged periods of time. These facts underline the importance of inclusion of an appropriate ABL model in any pollutant turbulent transport and dispersion package aimed at modelling long-range transport and diffusion phenomena.

The ABL model utilised in LED is driven by the following meteorological variables: 1) the geostrophic wind vectors $\vec{v}_g$ 2) the potential temperature ϑ_H at the top of the ABL; 3) surface temperature ϑ_s which can be calculated from the energy balance equation or taken from observation or numerical weather forecast model. From these external to ABL meteorological variables and the local parameters: the Coriolis parameter – f, the roughness parameter – z_0, the buoyancy parameter – $\beta = g/\overline{\vartheta}$, the following non-dimensional external parameters – Rossby number (Ro) and external stratification parameter (S) can be composed:

$$Ro = \frac{|v_g|}{fz_0} \quad \text{and} \quad S = \frac{\beta(\vartheta_H - \vartheta_s)}{f|v_g|}. \tag{2}$$

They uniquely define the turbulent regime in a horizontally homogeneous ABL. The details of the ABL model are presented in [10].

2.4 Atmospheric chemistry model

The major anthropogenic pollutants in the atmosphere are sulphur, nitrogen and hydrocarbon compounds. In this model only sulphur and nitrogen oxide chemical transformations are modelled, because their abundance and relatively long residence times in

the atmosphere. They are also the major reason for the formation of dry and wet acidic deposition.

The most important mechanism for the formation of acid deposition is the direct transformation of sulphur dioxide to sulphate:

$$SO_2 \xrightarrow{k_1} SO_4^{2-}, \tag{3}$$

where $k_1(t,r)$ is the constant of transformation which is a function of time and space.

The chemical transformations which NO and NO_2 undergo are rather complicated. Smog chamber measurements of the typical reactions of NO compounds show that 90% of them result in formation of NO, NO_2, PAN (Peroxyacetyl nitrate) and NO_3. This allows the chemical transformations of these five components to be included in the model. The equations describing the rate of transformation of the nitrogen compounds due to chemical and physical processes are (see [1]):

$$\begin{aligned}
\frac{d}{dt}[NO_2] &= -k_2[NO_2] + k_4[PAN], \\
\frac{d}{dt}[PAN] &= 0.5k_2[NO_2] - (0.5k_3 + k_4)[PAN], \\
\frac{d}{dt}[NO_3] &= 0.1(k_2[NO_2] + k_3[PAN]), \\
\frac{d}{dt}[HNO_3] &= 0.4(k_2[NO_2] + k_3[PAN], \\
0 &= [NO_2] - k_5[NO].
\end{aligned} \tag{1}$$

where k_2, k_3, k_4 and k_5 are the rates of chemical transformation as summarized in Table 1. The equilibrium of NO and NO_2 reflects the photolysis of NO_2 to NO and the photo and thermal pathways of NO to NO_2 conversion. The rate equations shown in equations (4) are linear. The transformation constants can be a function of time and space. The chemical reactions in the model are calculated for every puff at every time step after the completion of the transport and diffusion processes.

Table 1 – The rates of chemical transformation

	$k_1(s^{-1})$	$k_2(s^{-1})$	$k_3(s^{-1})$	$k_4(s^{-1})$	$k_5(s^{-1})$
Day	10^{-6}	$2.8\,x\,10^{-5}$	$2.8\,x\,10^{-5}$	0	2
Night	10^{-6}	$5.6\,x\,10^{-6}$	0	$5.6\,x\,10^{-6}$	50

2.5 Surface roughness

The surface roughness parameters utilized in the LED model conforms to a 0.5 degree spatial resolution Cartesian grid, inferred from the ecosystem database (see Fig. 2). The roughness parameters (z_0) utilized for the specific modelling domain in LED were generated and obtained from the Max-Planck Institute, Mainz, Germany. A detailed methodology on the generation of the roughness parameters can be found in [6].

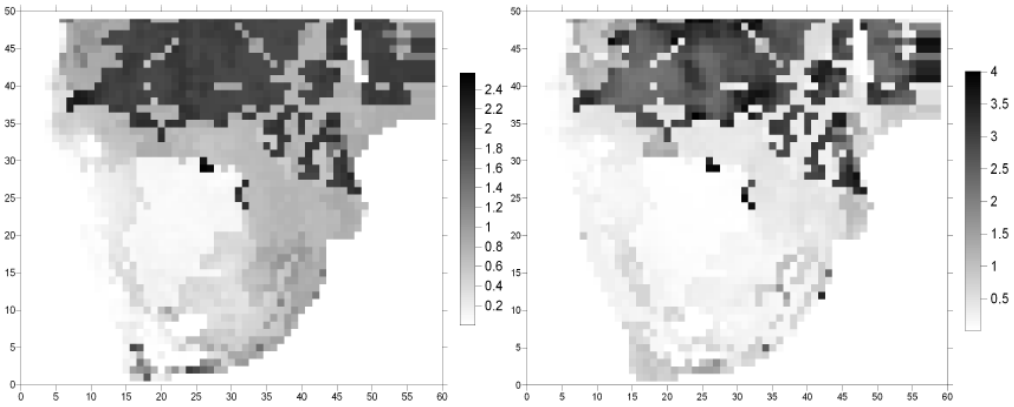

Fig. 2 – Surface roughness lengths z_0 (meters) for January (left) and July 2000 (right) for the study domain.

2.6 Emission Database

The emission database adapted for utilization in the LED model is a customized version of the emissions inventory developed in [4], in the framework of the SAFARI 2000 science initiative (see Fig. 3).

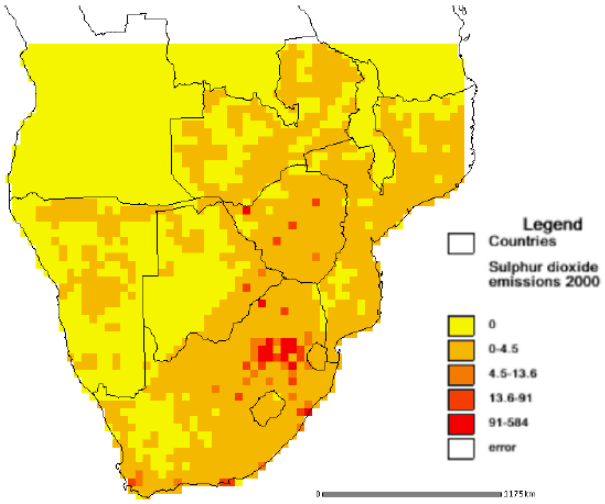

Fig. 3 – Sulphur dioxide (SO_2) emissions summed over all sectors for 2000. Units in Gg/annum.

2.7 Meteorology

The meteorological data utilized for input in the LED model is taken from the short-range forecasting ETA model routinely run by the South African Weather Service (SAWS). The ETA model outputs provided by the SAWS are ASCII map images (0.5 degree) for each of 51 meteorological parameters at 12 hour intervals. These ASCII map images are based on a 79 by 133 grid, 53°S to 9°S, 13°W to 53°E, 0.5 degree resolution.

Parameters available include geopotential height, temperature, potential temperature, dew point temperature, specific humidity, relative humidity, u and v wind components, cloud cover and pressure vertical velocity.

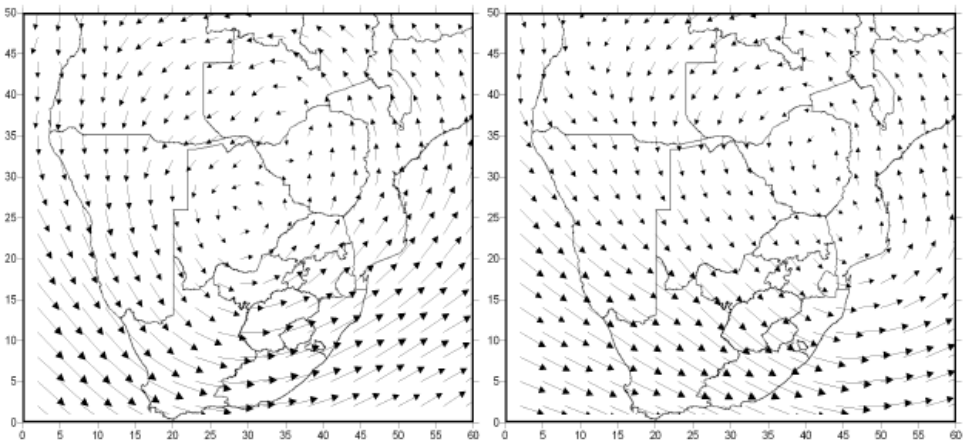

Fig. 4 – Geostrophic wind vectors on 700 hPa for 15 August 2000 at 00:00 (left) and 12:00 (right).

Figure 4 shows a major peculiarity of the winter circulation over the Southern Africa. The anti-cyclonic circulation persists for several days to week(s) leading to significant increase of the pollutant's concentration.

3 Results

The LED model was run for each month during 2000 using the relevant meteorological data, and the converted emission database included in [4]. It gives output for the time-space distribution of concentration and deposition fields of sulphur and nitrate compounds (Fig. 5 to Fig. 8) as well as the pH value of precipitation.

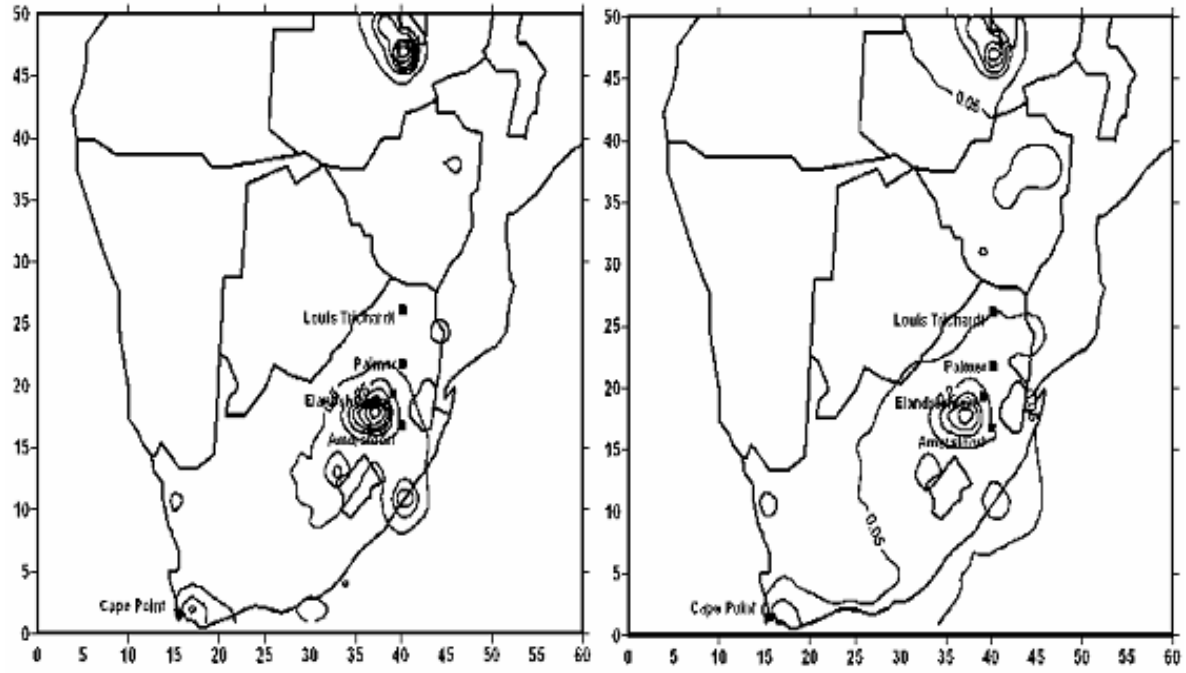

Fig. 5 – Mean ambient SO_2 concentrations ($\mu g.m^{-3}$) for the winter season during 2000 (left panel) and accumulated dry deposition, SO_x as S ($kg.ha^{-1}(3.months)^{-1}$) right panel.

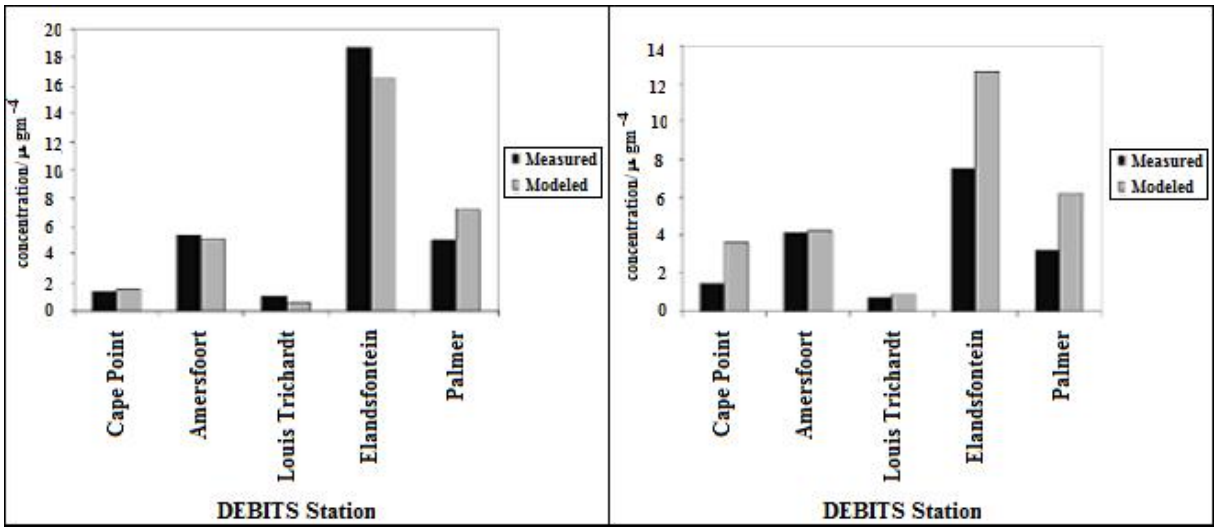

Fig. 6 – Annual modelled versus measured concentrations for the Deposition of Biogeochemical Important Trace Species (DEBITS) stations for the year 2000 – SO_2 (left panel), NO_2 (right panel).

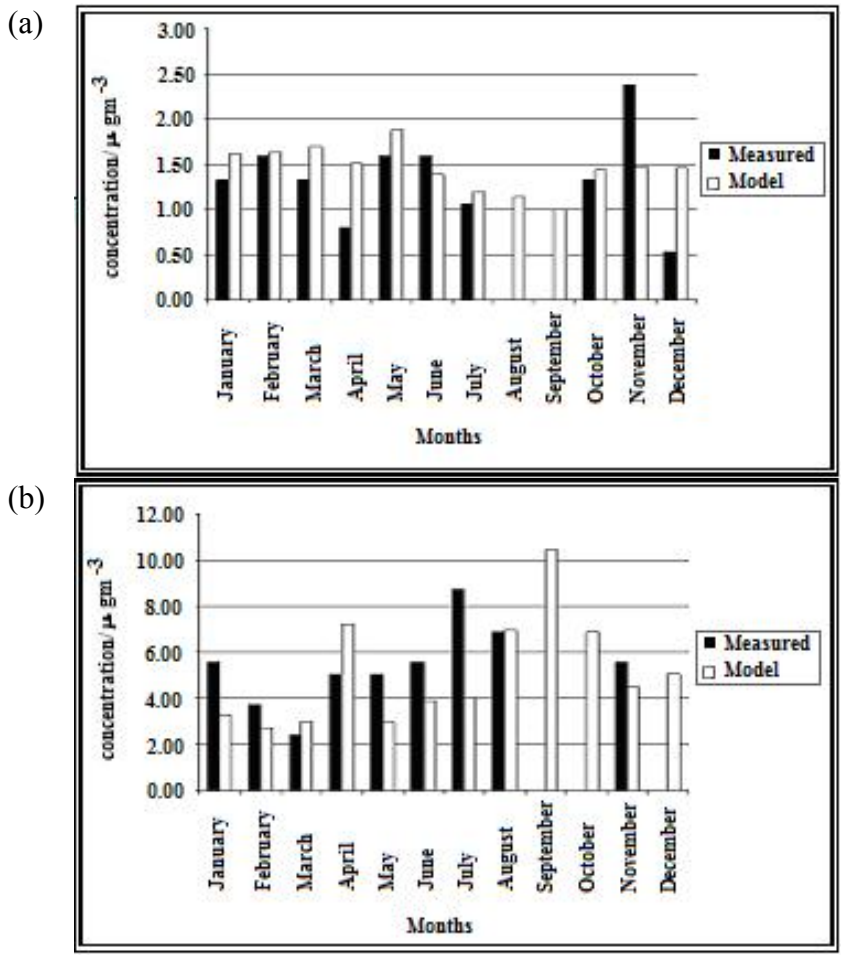

Fig. 7 – Monthly modelled SO_2 versus measured A. Cape Point station B. Amersfoot station

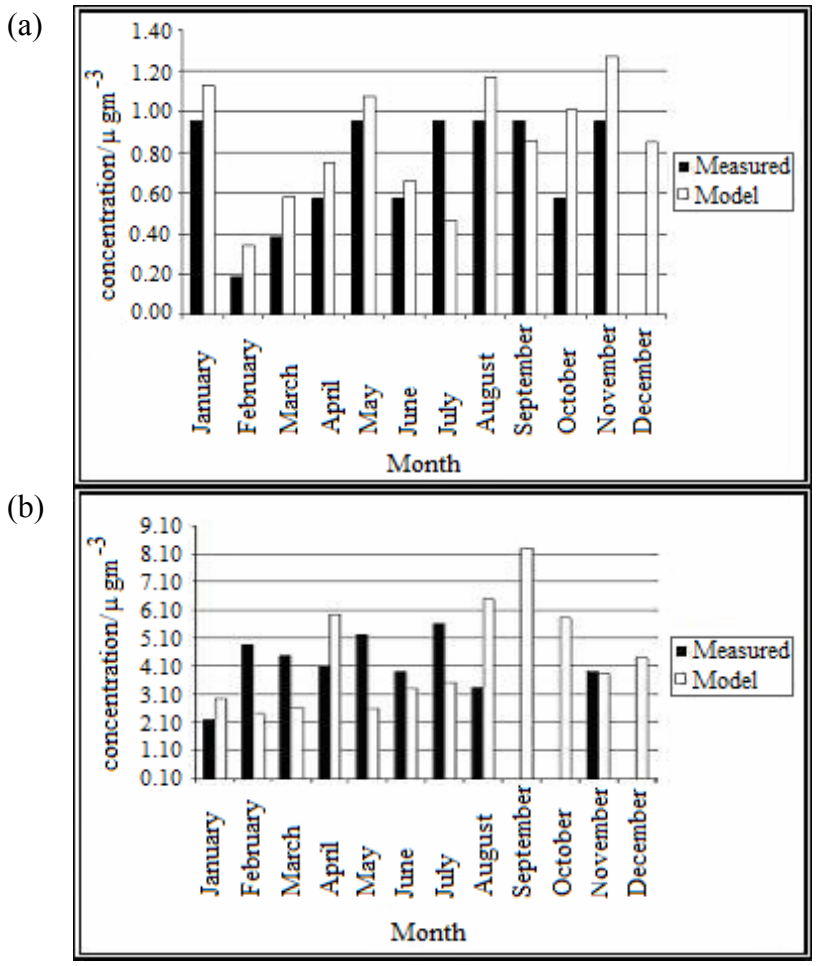

Fig. 8 – Monthly modelled NO_2 versus measured A. Louis Trichardt B. Amersfoot station.

Monthly runs for 2000 for all individual countries in the modelling region were executed with the LED model. The monthly deposition results can be used to obtain quantities on a country-to-country basis.

Table 2 – Annual country-to-country dry deposition matrix of SO_x as S for 2000

	RECEIVER									
EMITTER	Ang	Bot	Mal	Moz	Nam	Ocn	RSA	Zam	Zim	Total
Ang	96.61 4.55×10^{2}	0.01 4.85×10^{-2}	0.00 0.00	0.00 0.00	2.85 1.34×10^{1}	0.35 1.66	0.00 0.00	0.18 8.48×10^{-1}	0.00 0.00	100 -
Bot	3.50 2.56×10^{2}	32.58 2.38×10^{4}	0.15 1.13×10^{2}	4.77 3.49×10^{3}	2.76 2.02×10^{2}	4.91 3.59×10^{3}	38.08 2.78×10^{4}	3.47 2.53×10^{3}	9.77 7.15×10^{3}	100 -
Mal	0.53 8.05×10^{-1}	0.17 2.61×10^{-1}	10.67 1.63×10^{1}	78.72 1.20×10^{2}	0.13 1.93×10^{-1}	0.30 4.63×10^{-1}	0.14 2.11×10^{-1}	8.56 1.30×10^{1}	0.78 0.19	100 -
Moz	0.07 2.68	1.20 4.49×10^{1}	1.94 7.27×10^{1}	50.81 1.90×10^{3}	8.04 3.01×10^{2}	27.95 1.05×10^{3}	7.81 2.92×10^{2}	0.35 1.32×10^{1}	1.83 6.86×10^{1}	100 -
Nam	16.68 2.90×10^{2}	3.51 6.11×10^{1}	0.00 1.12×10^{-3}	0.70 1.22×10^{1}	75.88 1.32×10^{3}	2.13 3.70×10^{1}	1.05 1.82×10^{1}	0.02 2.70×10^{-1}	0.04 6.64×10^{-1}	100 -
Ocn	0.00 0.00	0.00 0.00	0.00 0.00	0.00 0.00	0.00 0.00	0.00 0.00	0.00 0.00	0.00 0.00	0.00 0.00	0.00 -
RSA	1.68 1.47×10^{4}	6.88 6.00×10^{4}	0.10 8.92×10^{2}	5.23 4.56×10^{4}	2.00 1.74×10^{4}	12.41 1.08×10^{2}	68.82 6.00×10^{2}	1.15 1.00×10^{4}	1.72 1.50×10^{4}	100 -
Zam	9.37 3.90×10^{2}	4.51 1.87×10^{3}	0.83 3.47×10^{2}	4.08 1.69×10^{3}	2.56 1.07×10^{3}	0.83 3.46×10^{2}	1.37 5.72×10^{2}	57.47 2.39×10^{4}	18.97 7.89×10^{2}	100 -
Zim	4.52 1.22×10^{2}	4.49 1.21×10^{3}	1.53 4.13×10^{2}	22.53 6.00×10^{3}	1.71 4.62×10^{2}	1.20 3.23×10^{2}	1.74 4.69×10^{2}	17.88 4.83×10^{3}	44.40 1.20×10^{4}	100

Top value: Percentage of total deposition received. Bottom value: tons.annum^{-1} received.

Tables 2 and 3 summarize LED results for the country-to-country dry deposition matrices, based on the country-specific emissions. The top values in both Tables indicate the percentage deposition received from the specified emitter indicated on the left hand side in the matrix. Therefore, every top horizontal line represents the partition of the deposition to its own and the other countries. It is obvious that the sum of the partition percentage quantities should add up to 100%. The bottom values in the horizontal lines are the deposition quantities (percentages) expressed in tonnes per annum. The vertical column drawn on the right hand side for each specific receiver country in Table 3 contains the percentage contribution to the deposition from the receiver countries. Again the sum of these percentages adds up to 100%.

Table 3 – Annual country-to-country dry deposition matrix of SO_x as S for 2000

	RECEIVER																					
EMITTER	Ang		Bot		Mal		Mog		Nam		Ocn		RSA		Zam		Zim		Total
Ang	96.61	-	0.01	-	0.00	-	0.00	-	2.85	-	0.35	-	0.00	-	0.18	-	0.00	-	1.00
	-	1.97	-	0.00	-	0.00	-	0.00	-	0.06	-	0.00	-	0.00	-	0.00	-	0.00	-
Bot	3.50	-	32.58	-	0.15	-	4.77	-	2.76	-	4.91	-	34.08	-	3.47	-	9.77	-	100
	-	11.09	-	27.19	-	6.11	-	5.93	-	8.93	-	3.16	-	4.43	-	6.14	-	16.93	-
Mal	0.53	-	0.17	-	10.67	-	78.72	-	0.13	-	0.30	-	0.14	-	8.56	-	0.78	-	100
	-	0.00	-	0.00	-	0.88	-	0.20	-	0.00	-	0.00	-	0.00	-	0.03	-	0.00	-
Mog	0.07	-	1.20	-	1.94	-	50.81	-	8.04	-	27.95	-	7.81	-	0.35	-	1.83	-	100
	-	0.01	-	0.05	-	3.92	-	3.23	-	1.33	-	0.92	-	0.05	-	0.02	-	0.16	-
Nam	16.08	-	3.51	-	0.00	-	0.70	-	75.88	-	2.13	-	1.05	-	0.02	-	0.04	-	100
	-	1.26	-	0.07	-	0.00	-	0.02	-	5.85	-	0.03	-	0.00	-	0.00	-	0.00	-
Ocn	0.00	-	0.00	-	0.00	-	0.00	-	0.00	-	0.00	-	0.00	-	0.00	-	0.00	-	100
	-	0.00	-	0.00	-	0.00	-	0.00	-	0.00	-	0.00	-	0.00	-	0.00	-	0.00	-
RSA	1.68	-	6.88	-	0.10	-	5.23	-	2.00	-	12.41	-	68.82	-	1.15	-	1.72	-	100
	-	63.49	-	68.94	-	48.13	-	77.40	-	77.06	-	56.29	-	16.36	-	24.21	-	35.59	-
Zam	9.37	-	4.51	-	0.83	-	4.08	-	2.56	-	0.82	-	1.37	-	57.47	-	18.97	-	100
	-	16.88	-	2.16	-	18.71	-	2.88	-	4.72	-	0.30	-	0.09	-	57.88	-	18.74	-
Zim	4.52	-	4.49	-	1.52	-	2.53	-	1.71	-	1.26	-	1.74	-	17.88	-	44.40	-	100
	-	5.29	-	1.40	-	22.26	-	19.34	-	2.05	-	0.28	-	0.07	-	11.70	-	28.51	-
Total	-	1.00	-	1.00	-	1.00	-	1.00	-	1.00	-	1.00	-	1.00	-	1.00	-	1.00	-

Top value: Percentage of total deposition received.
Bottom value: Origin of deposition load in percentage.

4 Discussions

The results obtained with LED, which are the first for the African continent south of the equator, clearly demonstrate that the phenomena of long-range transport of air pollutants is a serious, complex and significant problem for the countries in the southern African region.

LED model results for ambient concentrations, as well as deposition fields were produced for all months during the year 2000, and compared with the available experiment data at the DEBITS sites. Data obtained for the evaluation were in the framework of SAFARI 2000 research campaign. However, the ground measurements needed for the evaluation of LED were not sufficient due to the small number of observational points (5), and geographical locations which do not fully comply with the WMO criteria for baseline regional air quality stations.

Despite these inherent difficulties of not having a complete set of experimental data for the evaluation process, the comparison with model results give enough evidence that LED produce reliable results. The annual quantities compare quite accurately. The bigger variation in differences of the monthly quantities is also within the acceptable range.

The results for the deposition fields of pollutants indicate that impacts from highly industrial countries in the region may pose significant risks to developing countries, which relies for example on agriculture as a major contributor to the specific country's gross domestic product. The LED model supplies objective data, which lays the foundation for the development of all-inclusive regional air quality management plans. The implementation of such a management plan will be obviously beneficial to all countries in the region. The results

obtained from this modelling scenario highlight the complexity of trans-boundary air pollutant transport, and its serious developmental consequences, as well as the availability of reliable data for modelling as well as validation purposes.

5 Summary

The model results obtained with the Southern Hemisphere version of the LED model, which incorporates ABL model and chemical scheme, give assurance that it can be used as a diagnostic and prognostic tool for air pollution studies at different time and space scales. The comparison with the available experimental data demonstrates that the results are reliable. For example, the values of the monthly average concentrations fields are of reasonable order of magnitude and compare favourably with the measured values in the three DEBITS stations. The flexibility of the model is demonstrated by the calculation of the country to country deposition matrix that can be used as an effective planning tool. The results are expected to improve by upgrading the ABL model on the basis of the contemporary understanding and parameterization of the convective process in the tropics which is dominated by non-local turbulent transport. This also applies to taking into account the baroclinicity effects on the ABL dynamics.

There are several projects undertaken to be studied with the model, namely, runs with the natural emissions (vegetation, forest, soils) in order to partition the contribution of anthropogenic and natural sources to the pollution in the region; study the formation of ozone over the tropics; quantify the pollution episodes during a persistent gyre (anticyclonic) circulation and the fluxes of pollutants to the adjacent oceans and continents.

Acknowledgments. The study presented in the paper was completed in the framework of the SAFARI 2000 science initiative and authors have benefited from the scientific programme goals and discussions with the entire international research team.

References

1. *Brodzinsky, R., B. Cantrell, R. Endlich and C. Bhumralkar* (1984) A long range air pollution transport model for Eastern North America-II Nitrogen oxides. Atmospheric Environment, Vol. 18, No. 11, pp. 2361–2366.
2. *Djolov, G., D. Yordanov and D. Syrakov* (1987) Modelling the long-range transport of air pollutants with atmospheric boundary layer chemistry. Boundary-Layer Meteor., Vol. 41, pp. 407–416.
3. *Endlich, R., K. Nit., R. Brodzinsky and C. Bhumralkar* (1984) A long-range air pollution transport model for Eastern North America-I Sulphur Oxides. Atmospheric Environment, Vol. 18, No. 11, pp. 2345–2360.
4. *Fleming, G., and M van der Merwe* (2000) Spatial Desegregation of Greenhouse Gas Emission Inventory Data for Africa South of the Equator. ESRI. [Online].
5. *Fourie, G.* (2002) Air Pollution Modelling Needs in the Sasol Environment. Sastech R&D – Research Report, Sasol Technology Research & Development, Sasolburg, South Africa, 24 pp.
6. *Ganzeveld, L., J. Lelieveld., F. Dentener, M. Krol and G. Roelofs* (2002) Atmosphere biosphere trace gas exchanges simulated with a single-column model. J. Geophys. Res., 107, NO D16., 10.1029/2001JD0001289.
7. *Ludwig, L., L. Marufu., B. Huber, M. Andreae and G. Helas* (2003) Domestic Combustion of Biomass fuels in developing countries: A major source of atmospheric pollutants. Journal of Atmospheric Chemistry, Vol. 44, pp. 23–37.

8. *Pienaar, J., and G. Helas* (1996) The kinetics of chemical processes affecting acidity in the atmosphere. South African Journal of Science, Vol. 92, pp. 128–132.
9. *Syrakov, D., G. Djolov and D. Yodanov* (1983) Incorporation of planetary layer dynamics in a numerical model of long-range air pollutant transport. Boundary-Layer Meteor., Vol. 26, pp. 1–13.
10. *Yordanov, D., D. Syrakov and G. Djolov* (1983) A barotropic planetary boundary layer, Boundary-Layer Meteor., Vol. 25, pp. 363–373.

Моделирование дальнего переноса и химических превращений примеси в Южной Африке

Аннотация. *В статье представлены результаты расчетов по атмосферной модели дальнего переноса примеси. Данная модель была разработана специально для условий Южного полушария. В модели используется смешанное (совместное эйлерово и лагранжево) описание переноса и распространения примесей, вычисление их химических трансформаций, сухого и мокрого осаждений, а также показатель кислотности (pH) дождей.*

Ключевые слова: *дальний перенос загрязняющих веществ, пограничный слой атмосферы, выброс, шероховатость подстилающей поверхности, метеорология, атмосферная химия, турбулентная диффузия.*